Available online at www.sciencedirect.com
SCIENCE DIRECT®
Advances in Water Resources 28 (2005) 345–358
Advances in Water Resources
www.elsevier.com/locate/advwatres

On the form of the momentum equation for shallow water models based on the generalized wave continuity equation

Kendra M. Dresback *, Randall L. Kolar, J. Casey Dietrich

School of Civil Engineering and Environmental Science, University of Oklahoma, Norman, OK 73019, USA

Received 30 May 2004; received in revised form 27 October 2004; accepted 5 November 2004

Abstract

Nearly all generalized wave continuity (GWC)-based models utilize the velocity-based, non-conservative form of the momentum equation to obtain the depth-averaged changes in velocity. It has been hypothesized that a flux-based, conservative form of the momentum equation may improve accuracy and stability. Herein, we study the impact of the choice of dependent variable and form of the momentum equation in a GWC-based finite element shallow water model. The impact of this change on mass balance, stability, and accuracy (spatial and temporal) is rigorously assessed, first for 1D barotropic flows and then for 2D barotropic flows in a variety of basins. Both 1D and 2D results indicate that the conservative form improves mass balance on both global and local scales, with the most significant gains found in local mass balance in areas with steep bathymetry gradients. This is also the region where the conservative form shows an increase in local spatial accuracy. Taylor series analysis and numerical simulations indicate a strong correlation between local spatial truncation errors and local mass balance errors. Stability, temporal accuracy and global spatial accuracy do not show statistically significant changes between the two algorithms in both 1D and 2D studies.

Keywords: Shallow water equations; Finite elements; Generalized wave continuity; Conservative momentum; Non-conservative momentum; Depth-averaged equations

1. Introduction

Shallow water equations are used to describe the hydrodynamic behavior of oceans, estuaries, coastal regions, lakes and impoundments. The depth-averaged versions of the conservation of mass and momentum form the basis of the shallow water equations in their native or primitive form. Early finite-element based shallow water models that utilized the primitive form of the shallow water equation suffered from stability problems due to spurious oscillations in the solutions. In 1979, Lynch and Gray [18] introduced the wave continuity equation (WCE), which eliminated the spurious oscillations in the solution without having to dampen the solution numerically or artificially. Kinnmark [11] determined in 1986 that there was no loss in the propagation characteristics of the wave continuity equation if a numerical parameter, G, was introduced, thus obtaining the generalized wave continuity (GWC) equation (see Section 2 for more details on the GWC).

Finite element shallow water models based on the GWC equation may be prone to errors in local mass conservation [1,11–14,19], as measured by direct integration of the continuity equation (also referred to in the literature as a "finite volume" approach). We acknowledge the recent work of Hughes et al. [10] and Berger and Howington [2], who argue that continuous Galerkin finite elements are locally conservative, provided that the external flux is computed in a method consistent with

* Corresponding author. Tel.: +1 405 325 5218; fax: +1 405 325 4217.
E-mail addresses: dresback@ou.edu (K.M. Dresback), kolar@ou.edu (R.L. Kolar), caseydietrich@ou.edu (J.C. Dietrich).

0309-1708/$ - see front matter © 2004 Elsevier Ltd. All rights reserved.
doi:10.1016/j.advwatres.2004.11.011

the discretization, e.g., a weighted residual boundary integral. A full comparison of the two approaches (finite volume vs. weighted residual) is beyond the scope of this work, but our experience with the "consistent flux" approach of Hughes and Berger indicates it is not sensitive to grid resolution (mass balance error does not change with decreasing resolution). Hence, it does not provide a measure of solution accuracy. On the other hand, the finite volume approach can provide such information, which is an issue we explore in Section 4.5.

Keeping with the finite volume method of computing mass balance errors, we note that these errors are particularly large for highly non-linear flows, which include shallow, converging sections around barrier islands and flood waves propagating onto dry land [12,14]. Kinnmark provided the first theoretical analysis of the mass conserving properties of the GWC equation [11]. The GWC equation, which is part of a class of derivative equations, allows for a larger solution space than does the primitive form of the equations. In order to restrict this solution space, Kinnmark determined that several auxiliary conditions must be met. He obtained the auxiliary conditions by determining the equivalence between the primitive form of the shallow water equations, including the conservative form of the momentum and continuity equations, and other formulations, such as the wave continuity equation. Kinnmark determined that the continuity equation, including its boundary conditions, must be exactly satisfied during spin-up in order for mass to be conserved. However, because of roundoff errors and other noise that occurs during spin-up of a numerical model, this cannot always be guaranteed. Supporting this observation were Walters and Carey, who hypothesized that the vanishing of the derivative of the continuity equation with respect to time is not sufficient to ensure that mass is conserved [20]. Because the first condition cannot always be satisfied, Kinnmark investigated two other auxiliary conditions, of which one must be met. First, if the non-conservative momentum (NCM) equation is used, then $G > \nabla \cdot \mathbf{v}$ (where G is the GWC equation numerical parameter and $\mathbf{v}$ is the depth-averaged velocity field). In practice, because an upper bound exists on G above which spurious modes are generated, one cannot guarantee that this requirement is satisfied for a time-dependent velocity field. Second, if the conservative form of the momentum equation (CM) is used, then $G > 0$, which is a condition that can always be met [11].

Aldama et al. analyzed mass conservation of the GWC and NCM equations in their continuous and discrete forms, using both a Taylor–Frechet and Fourier series analysis [1]. In their analysis of the discrete form of the equations, they found that the GWC formulation is not consistent with the mass conservation principle, and the mass conservation error was proportional to e^{-Gt}. For a given time, as $G \to \infty$, the error approaches zero. A balance between the choice of G and the amount of residual error must be obtained, because, as $G \to \infty$, the GWC equation approaches the primitive form of the continuity equations and produces spurious oscillations.

In concurrent studies, Kolar et al. [12–14] examined the sensitivity of mass conservation to the G parameter and boundary conditions. In two of these studies, they determined that implementing mass conserving boundary conditions improves global mass balance errors without increasing G and improves local mass balance errors with a lesser value of G [12,13]. Also, Lynch and Holboke analyzed the mass conservative boundary conditions in a 3D framework and determined the boundary conditions could be implemented differently to improve the global mass conservation; however, local mass conservation was not analyzed [19].

In another study, Kolar et al. also examined recasting the advective term in the GWC equation into non-conservative form so that it mimics the formulation in the NCM equation [14]. They found that global mass conservation is improved; however, local mass conservation errors persisted. In summary, they recommended that GWC models match the form of the advective terms and that the ratio of $G/\tau_{\max}$ is $1 \leqslant G/\tau_{\max} \leqslant 10$, where τ is the bottom friction coefficient as determined from a quadratic friction law:

$$\tau = C_{\mathrm{f}} \frac{\sqrt{(u^2 + v^2)}}{H} \tag{1}$$

and $\tau_{\max}$ is the largest magnitude of τ over the spatial domain. In Eq. (1), u and v are depth-averaged velocities, H is the total water depth, and C_{f} is the bottom friction parameter. When the ratio falls within this range, the non-linear constituent errors and the global and local mass balance errors are both minimized without introducing spurious modes [14].

Several studies have examined the relationship between the meshing criteria and grid convergence [3,8,9,16]. In particular, Hagen et al. [8,9] developed a meshing technique that examines the local truncation error associated with the linearized form of the NCM equation. This study showed that refinement in areas where truncation error is large (e.g., in areas where steep bathymetry gradients occur) and coarsening in areas where truncation error is small, improves the overall accuracy of the solution without increasing the computational burden. These areas correspond to where the velocity-based NCM solution changes rapidly.

From the literature cited above, we observe the following about NCM-based GWC equation models: (1) local mass balance errors (as measured by direct integration of the continuity equation) and instabilities can occur, particularly in regions with highly non-linear flows; (2) numerical and analytical studies demonstrate that the problem can be lessened, but not eliminated, by proper choice of G, by reformulating the advective

terms, and by proper treatment of the boundary conditions; and (3) high levels of grid refinement are needed in areas with steep bathymetry gradients to minimize truncation errors. Based on these observations, we hypothesize that changing to the conservative form of the momentum equation, which is flux-based and not velocity-based, will improve both global and local mass conservation, eliminate the need to reformulate the advective term between the governing equations, and lessen the need for extensive refinement in areas with steep bathymetry gradients due to flux varying more slowly than velocity in these regions. Also, use of the conservative form of the momentum equation makes it more natural to bring in flux boundary conditions and facilitates coupled models (e.g., discontinuous and continuous Galerkin methods [4,5]). Thus, the primary objective of this paper is to assess the impact of the conservative form of the momentum equation on mass conservation, stability, temporal and spatial accuracy for GWC-based finite element models. Numerical simulations will be conducted with the ADCIRC (ADvanced CIRCulation model [17]) family of models.

2. Background

Testing of the conservative form of the momentum equation (CM) was done with both the 1D and 2D version of ADCIRC. If the operator L represents the primitive continuity equation and $\mathbf{M}_c$ the conservative form of the momentum equation, then the GWC equation is obtained from the following operation:

$$\frac{\partial L}{\partial t} + GL - \nabla \cdot \mathbf{M}_c = 0 \tag{2}$$

In Eq. (2) G controls the relative weight of the primitive continuity equation, such that if $G \to 0$, the equation becomes a pure wave continuity equation, whereas if $G \to \infty$, the equation is a pure primitive continuity equation.

In the 1D version, we neglect atmospheric and tidal potential forcings and assume the eddy viscosity is constant; the standard form of the ADCIRC model equations (GWC, NCM and CM, Eqs. (3)–(5), respectively) are as follows:

$$\frac{\partial^2 \zeta}{\partial t^2} + G\frac{\partial \zeta}{\partial t} - q\frac{\partial G}{\partial x} - \frac{\partial}{\partial x}\left[\frac{\partial (qu)}{\partial x} + (G-\tau)q + gH\frac{\partial \zeta}{\partial x} - \varepsilon\frac{\partial^2 q}{\partial x^2}\right] = 0 \tag{3}$$

$$\frac{\partial (u)}{\partial t} + u\frac{\partial (u)}{\partial x} + \tau u + g\frac{\partial \zeta}{\partial x} - \frac{\varepsilon}{H}\frac{\partial^2 (Hu)}{\partial x^2} = 0 \tag{4}$$

$$\frac{\partial (q)}{\partial t} + \frac{\partial (qu)}{\partial x} + \tau q + gH\frac{\partial \zeta}{\partial x} - \varepsilon\frac{\partial^2 q}{\partial x^2} = 0 \tag{5}$$

where $q = Hu$ is the depth-averaged flux, u is the depth-averaged velocity, $\tau = C_f(|u|/H)$, ε is the eddy viscosity, t is time, ζ is the elevation of the water surface above the datum, x is distance, G is the GWC numerical parameter and $H = h + \zeta$ is total water column depth.

In the 1D studies with the GWC–NCM model, the advective term in the GWC equation takes on two different forms, consistent or inconsistent. The inconsistent form is developed from Eqs. (3) and (4) because the advective term in the GWC equation is in conservative form and the advective term in the NCM equation is in non-conservative form. In the consistent formulation, the advective term in the GWC equation is altered to the non-conservative form (as reported in [14]) by introducing the primitive continuity equation so that a second-order space derivative is replaced by a mixed space and time derivative.

Equations for the 2D ADCIRC model (GWC, NCM and CM, Eqs. (6)–(8), respectively) with a constant eddy viscosity are as follows:

$$\frac{\partial^2 \zeta}{\partial t^2} + G\frac{\partial \zeta}{\partial t} - \mathbf{q}\nabla \cdot G - \nabla \cdot \left\{\nabla \cdot (\mathbf{q}\mathbf{v}) + \mathbf{f} \times \mathbf{q} + (G-\tau)\mathbf{q} + H\nabla\left[\frac{p_a}{\rho} + g(\zeta - \alpha\eta)\right] - \mathbf{A} - \varepsilon\nabla^2(\mathbf{q})\right\} = 0 \tag{6}$$

$$\frac{\partial (\mathbf{v})}{\partial t} + \mathbf{v}\nabla \cdot (\mathbf{v}) + \tau\mathbf{v} + \mathbf{f} \times \mathbf{v} + \nabla\left[\frac{p_a}{\rho} + g(\zeta - \alpha\eta)\right] - \frac{\mathbf{A}}{H} - \frac{\varepsilon}{H}\nabla^2(H\mathbf{v}) = 0 \tag{7}$$

$$\frac{\partial (\mathbf{q})}{\partial t} + \nabla \cdot (\mathbf{q}\mathbf{v}) + \tau\mathbf{q} + \mathbf{f} \times \mathbf{q} + H\nabla\left[\frac{p_a}{\rho} + g(\zeta - \alpha\eta)\right] - \mathbf{A} - \varepsilon\nabla^2(\mathbf{q}) = 0 \tag{8}$$

New terms in these equations are as follows: $\mathbf{q} = H\mathbf{v}$ is the depth-averaged flux, $\mathbf{v}$ is the depth-averaged velocity, $\mathbf{f}$ is the Coriolis parameter, given by $2\Omega\sin\phi$, Ω is the angular velocity of the earth and ϕ is latitude, g is gravity, α is the earth elasticity factor, $\mathbf{A}$ is the wind stress on the water surface, η is the Newtonian equilibrium tidal potential, ρ is density, and p_a is barometric pressure.

In ADCIRC, linear finite elements are used for the spatial discretization, while for the temporal discretization, a three time-level scheme centered at k is used in Eqs. (3) and (6) and a two time-level scheme centered at $k + 1/2$ is used in Eqs. (4), (5), (7) and (8). Flux-based (CM equation) solutions are obtained by first solving Eq. (3) or (6) for the elevation change and then using Eq. (5) or (8), depending on 1D or 2D; in either case, new velocity values are obtained by dividing the nodal flux by the total water depth at that point. Velocity-based (NCM equation) solutions substitute Eq. (4) for (5) and Eq. (7) for (8). Ocean boundaries are treated as essential conditions in the continuity equation while flux boundaries are treated as natural in the continuity equation and

essential in the momentum equation. This implementation is often referred to as "conventional" treatment. In order to keep the focus on the form of the momentum equation, we did not examine alternative treatments.

3. Procedures

3.1. Mass conservation

In order to evaluate the changes to mass balance errors, we compare the accumulation of mass to the net flux of the mass leaving the element or domain by directly integrating the primitive continuity equation, as has been done in similar studies [14]. In brief, the nodal variables are expanded in space using their linear basis functions and integrated exactly, while the time integral is approximated with the trapezoidal rule. For details, we refer the reader to Ref. [14]. In this paper, we present the mass balance errors as the average absolute error over the simulation time. We average these errors over time for both local and global results. As noted in Section 1, we are purposely using the "finite volume" approach of checking mass balance because of the diagnostics it provides (see Section 4.5).

3.2. Stability

To evaluate stability heuristically, we obtain the maximum stable time step for a given simulation from the following procedures: (1) Find the maximum allowable time step with the NCM equation to the nearest five seconds; (2) Find the maximum allowable time step with the CM equation to the nearest five seconds; and (3) Compare the results from both equations and determine the percent change between the two results.

3.3. Accuracy

3.3.1. Temporal

In this study, we do not change the algorithm to approximate the time derivatives in the momentum equation; therefore temporal accuracy should not be influenced. To verify this, we looked at the global temporal accuracy and found that in neither 1D nor 2D did the change in the form of the momentum equation significantly influence the temporal accuracy convergence rates for any of the domains evaluated. This is also evident in the Taylor Series expansions of the discrete equations, in which both momentum equations are first order accurate in time for non-linear problems. (The full expansions are given in Ref. [7].)

3.3.2. Global spatial accuracy

Numerically, the "true solutions" for the 1D experiments were chosen by performing a grid convergence test where refinement of the grid occurred until a chosen convergence criterion (errors on the order of 10^{-6} m or m/s) was met. We then compared fine and coarse grid results to measure the errors, as expressed by L_2 and L_∞ norms. For the L_2 errors, we averaged these errors over time to provide one data value for every grid resolution studied.

3.3.3. Local spatial accuracy

For 1D, we utilized the same grid convergence procedures outlined under global accuracy to establish the "true solution". We then compared fine and coarse grid results to measure the errors, as expressed by the average nodal error over the number of tidal cycles. In this case, the errors were averaged over time but not over space so the results are shown on a nodal basis. For the 2D spatial accuracy experiments, Cumulative Area Fraction Error (CAFE) [16] plots provide information on local accuracy changes. CAFE plots produce absolute and relative errors between two simulations of the same domains with the same temporal resolution, but different spatial resolutions. A discussion of the CAFE plots and how to read them can be found in Refs. [6,9]. To develop CAFE plots for this study, we used the following steps: (1) Harmonic data is recorded for the NCM equation over several tidal cycles for both a coarse and fine spatial resolution; (2) Harmonic data is recorded for the CM equation over several tidal cycles for the same coarse and fine spatial resolution; (3) Absolute and relative errors are calculated for each form of the momentum equation; (4) Cumulative errors for both equations are computed; and (5) Results are plotted on the same graph to determine the percent area exceeding a certain criteria for convergence.

4. One-dimensional numerical experiments

4.1. Domains evaluated

Four 1D domains were used to examine the effects of the conservative form of the momentum equation: a constant bathymetry of 5 m (Fig. 1a); a parabolic bathymetry (Fig. 1b, also denoted "quadratic"), which has a rate of rise that varies as a second-order polynomial; the Western North Atlantic bathymetry (Fig. 1c, also denoted "eastcoast"), which is a 1D slice across the eastern United States continental shelf out into the deep Atlantic Ocean; and a sinusoidal varying bathymetry (Fig. 1d, also denoted "sinusoidal"). The sinusoidal bathymetry induces diverging and converging flow fields in a 1D setting. Each of the domains used the following simulation conditions: an eddy viscosity parameter of zero, a 1-m M_2 tidal forcing at the ocean boundary (a forcing that we have found through experience to produce critical responses in the system), and no normal

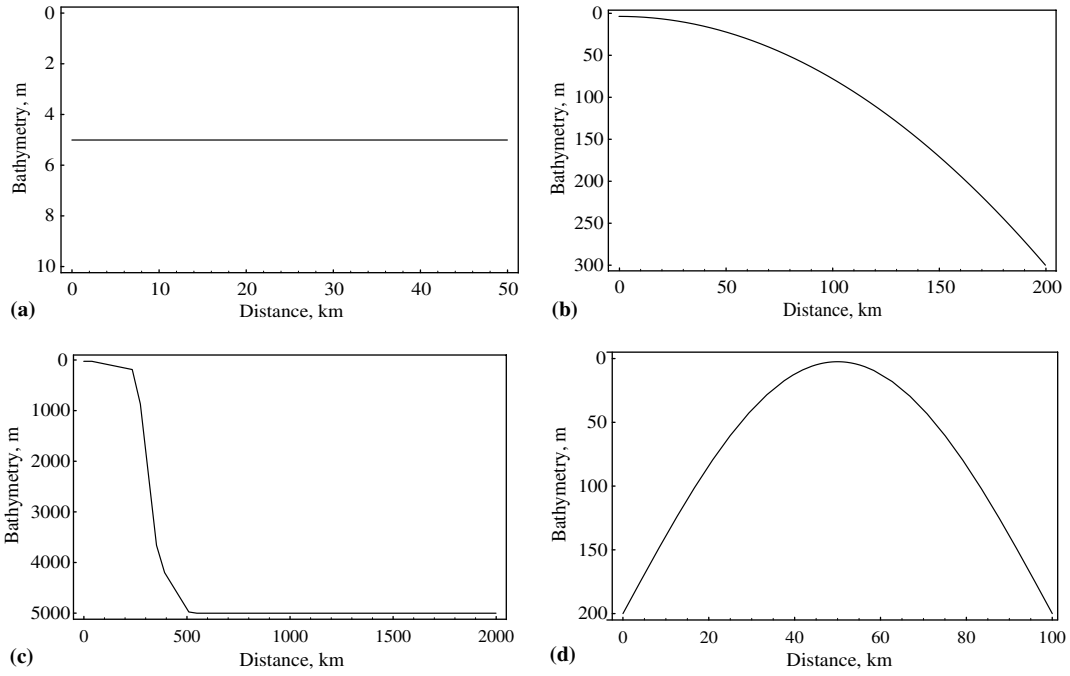

Fig. 1. Schematics of the 1D domains: (a) constant, (b) quadratic, (c) eastcoast and (d) sinusoidal.

flux at the land boundary. Maximum and minimum bathymetry values for the parabolic domain are 300 and 3 m, respectively; for the Western North Atlantic, the maximum and minimum bathymetry values are 5000 and 20 m, respectively; for the sinusoidal domain, the maximum and minimum bathymetry values are 200 and 2.5 m, respectively, with the minimum depth occurring in the center of the domain. In general, we used one of two different spatial discretization techniques, constant and variable, for these domains. In what follows, the $\lambda/\Delta x$ ratio is defined as

$$\frac{\lambda}{\Delta x} = \frac{\sqrt{gh} \times T}{\Delta x} \tag{9}$$

where h is the bathymetry, T indicates the period of the tidal constituent and Δx is the nodal spacing. For a constant spatial discretization of a domain, we divided the reach into N equal-sized elements, where N was chosen (see Table 1) to produce the desired $\lambda/\Delta x$ ratio for the M_2 wave in the shallowest (i.e., most critical) region. Of course, this means that in the deeper portions of these domains, the M_2 wave is even more finely resolved.

As for the variable spatial discretization, we keep the $\lambda/\Delta x$ ratio constant to determine the Δx values for all of the domains. In this method, the initial node is placed at the land boundary, the wavelength is determined from the nodal bathymetry, and then a Δx value is

Table 1
Meshing criteria for the 1D numerical experiments

Domain	Spacing criteria	Numerical experiments				
		Mass conservation		Spatial accuracy		Stability
		Global	Local	Global	Local	
Constant	Constant[a]	51	NA[b]	NA	NA	51
Quadratic	Constant	201	76[c]	Varies—11 to 1001	NA	201
Quadratic	Variable[d]	300	300	Varies—25 to 5000	NA	300
Eastcoast	Constant	201	101	Varies—11 to 2001	101, 201, 401, 801	201
Eastcoast	Variable	300	300	Varies—25 to 5000	300, 1200, 5000	300
Eastcoast	LTEA	NA	46	NA	46	NA
Sinusoidal	Constant	100	41	Varies—11 to 1001	NA	43
Sinusoidal	Variable	300	300	Varies—100 to 10,000	300, 1000, 5000	300

[a] Number of nodes is given for constant spacing.
[b] NA—experiments were not performed with this domain and nodal spacing.
[c] Chosen to have approximately same # of nodes as the variable spacing criteria.
[d] The $\lambda/\Delta x$ ratio is given for variable spacing.

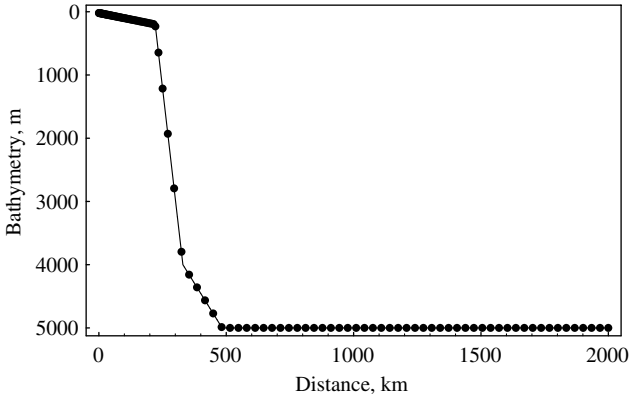

Fig. 2. Schematic of the $\lambda/\Delta x$ grid (black dots) that shows how the nodes are placed with the bathymetry shown in the background (line). Figure uses a $\lambda/\Delta x = 300$.

calculated from the ratio shown in Eq. (9). The next node is placed at this Δx distance from the land boundary. From a background grid of bathymetry, we determine the bathymetry at this location and use it to obtain the wavelength value. Then using the chosen $\lambda/\Delta x$ ratio, we determine the new Δx value, which is placed that distance from the previously defined node. Fig. 2 shows a schematic of a variable $\lambda/\Delta x$ grid and the placement of the nodes for the eastcoast domain using a $\lambda/\Delta x$ ratio of 300.

For one study, we also utilized another variable grid meshing criteria that is developed from a local truncation error analysis (LTEA) of the velocity-based non-conservative momentum equation. This meshing criteria, developed by Hagen et al. [8,9], places more nodes in the areas where high local truncation errors exist. These areas tend to be where there are steep topography changes, such as the continental rise in the eastcoast domain.

A summary of the meshing criteria for all of the 1D numerical experiments is provided in Table 1. For each of the 1D experiments, we indicate the nodal spacing technique used and the meshing criteria, which is either the number of nodes for constant nodal spacing or the $\lambda/\Delta x$ ratio for variable nodal spacing. Multiple values are included when the experiment called for multiple grids, such as an analysis of spatial accuracy.

4.2. Mass conservation

We first investigated the impact of the CM equation on mass conservation, an issue that has been noted to plague non-linear applications when measured using a finite volume approach [1,11–14,19] (also see second paragraph in Section 1). Experiments in this section utilize the procedures referenced in Section 3.1. In the studies herein, we computed mass conservation errors for the NCM equation using the following formulations: (1) the inconsistent form of the advective terms, which means the GWC equation advective terms are in conservative form and the NCM advective terms are in non-conservative form; and (2) the consistent form of the advective terms, which means the GWC equation and the advective terms in the NCM equation are in the non-conservative form (requires manipulation of the GWC equation, as reported in [14]). We evaluated the errors in global and local mass conservation for six M_2 tidal cycles for all domains utilizing a 5-s time step.

4.2.1. Global mass conservation

Fig. 3 presents the average absolute error in the global mass balance for the NCM and CM equations for all domains, using two types of meshing, constant (C) and variable (V). All parameter values are the same within each domain. Results show that adopting the CM equation improves global mass balance in most of the domains. Improvement in the global mass balance errors for the CM equation is less evident with the variable nodal spacing than with the constant nodal spacing (for a given domain); the latter shows up to two orders of magnitude improvement, except for the eastcoast domain. The behavior of the eastcoast results can be explained by noting the large percentage of the domain with deep bathymetry where the non-linear terms are not significant, thus the form of the advective terms is insignificant. (We will explore this issue further later in Section 4.5.) A consistent treatment of the advective terms (diagonals) partially offsets the mass balance improvement realized by the CM equation, thus indicating that both the form of the advective terms and the choice of dependent variable plays a role. This is explored further in Section 4.5.

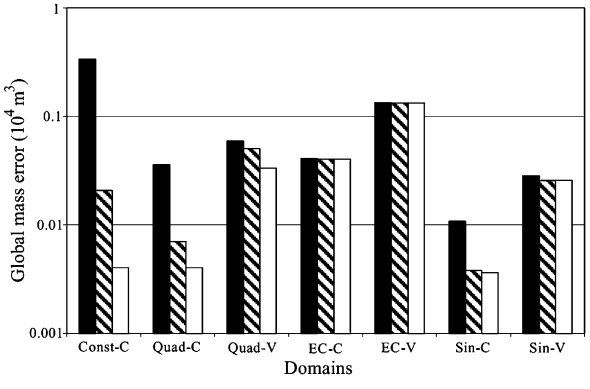

Fig. 3. Errors in the global mass conservation for all the domains; NCM equation—inconsistent GWC advective formulation (black), NCM equation—consistent GWC advective formulation (diagonals), CM equation (white). Abbreviations are Const—constant; Quad—quadratic; EC—eastcoast; Sin—sinusoidal; C—constant spatial discretization; V—variable spatial discretization.

4.2.2. Local mass conservation

For local mass conservation, we looked at two domains with steep bathymetry gradients: the eastcoast (Fig. 1c) and the sinusoidal (Fig. 1d). Both cases use constant and variable nodal spacing. Results using the variable nodal spacing are shown in Fig. 4. A schematic of the bathymetry for each domain is also shown by the short dashed line in the figure. In these experiments, we evaluated local mass balance errors for the NCM equation with the two forms of the GWC advective terms; the inconsistent form and the consistent form (see Section 2). As can be seen, the CM formulation provides a significant error reduction in areas where there is a steep bathymetry gradient. In contrast, we find that the NCM results show large local mass balance errors where a steep bathymetry gradient occurs, regardless of the treatment of the advective terms. For the eastcoast domain, we determined from numerical experiments that the grid spacing for the NCM simulation would have to be decreased by a factor of 20 (consistent advective terms) or 115 (inconsistent advective terms) in order to have the same level of local mass balance error as the CM equation.

In Fig. 4, note that the open boundary (element 107 in Fig. 4a and 40 in Fig. 4b) shows larger local mass balance errors than the land boundary, which corresponds to earlier findings for a "conventional" treatment of boundary conditions [14]. As mentioned, because this manuscript focuses on the form of the momentum equation, we did not revisit the boundary condition issue. Also, note that for the quadratic bathymetry (not shown), we observed a decrease in the local mass errors at the land boundary for the CM equation as compared to the NCM equation. Overall, the CM equation improves the local mass balance errors in the domains evaluated with the greatest gains seen in areas of steep bathymetry changes, which correspond to areas where the non-linear terms are dominant.

We also examined the influence of the type of spatial discretization (constant vs. variable node spacing) on local mass conservation. Similar results as given in Fig. 4 were found for constant nodal spacing using approximately the same number of nodes, but with higher differences between the local mass balance errors for the two forms of the momentum equations. For example in the eastcoast domain, the local mass balance errors increased by approximately 30% for the NCM equation in the area of the steep bathymetry change. In all cases, the local mass balance errors for the CM equation decrease as compared to the errors for NCM equation.

4.3. Spatial accuracy

4.3.1. Global spatial accuracy

We evaluated the CM algorithm's impact on global spatial accuracy following the procedures presented in Section 3.3.2. For the 1D experiments, we looked at two techniques of obtaining the "true solution", one based on the $\lambda/\Delta x$ ratio and one based on successively refining Δx on a uniform mesh by a factor of two. For the $\lambda/\Delta x$ approach, we found that a ratio of 5000 provided the desired convergence criteria for all the domains evaluated; while for the other method, we found that a resolution of $\Delta x = 61$ m for eastcoast domain, $\Delta x = 25$ m for the sinusoidal domain, and $\Delta x = 24$ m for the quadratic domain meets the convergence criteria. A cross comparison of these "true solutions" shows that the results were nearly identical, so the $\lambda/\Delta x$ ratio is used in the remainder of this subsection. The global spatial accuracy experiments used both constant and variable nodal spacing, with the ranges of grid refinement shown in Table 1, and a time step of 1 s. Results (not shown) from these domains produced similar convergence rates for both forms of the momentum equation. Therefore, no significant effect is seen on the global spatial accuracy results when utilizing the conservative form of the momentum equation.

4.3.2. Local spatial accuracy

Next, we looked at the CM algorithm's impact on local spatial accuracy following the procedures presented

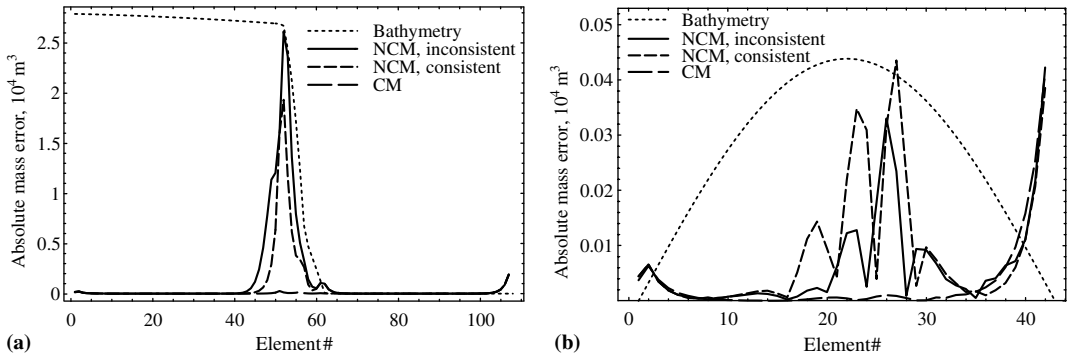

Fig. 4. Local mass conservation results for two formulations of the momentum equation for (a) eastcoast and (b) sinusoidal domains. Legend is shown in the figure. Note that the bathymetry is not to scale.

in Section 3.3.3. Based on the local mass conservation results, we focused on the eastcoast and sinusoidal domains, as these show the greatest change in local mass conservation errors. The "true solution" based on a uniform mesh was employed for both domains. The grid resolution parameters are shown in Table 1.

Results for the variable-spaced grids for these domains are shown in Fig. 5, with a schematic of the bathymetry shown by the shorter dashed lines. The figures indicate that the CM equation increases the local spatial accuracy, particularly along areas of steep topography changes. The highest error with the non-conservative form of the momentum equation occurs at the top of the continental shelf area for the eastcoast domain. In the sinusoidal domain, we find that the non-conservative momentum equation has higher local spatial errors before and after the bathymetry rise than the conservative momentum equation results; while, the conservative momentum equation shows an increase in error at the peak of the bathymetry. In Fig. 5b, it is interesting and important to note that the NCM local spatial errors shows a similar 3-peak pattern as the local mass errors of Fig. 4b. Note that both momentum equations show an error near the land boundary in both domains. Local accuracy results differ from global accuracy because the latter averages the errors over the domain, which tends to smooth out the local errors.

Finally, we looked at the interaction of the meshing criteria with the form of the momentum equation. In particular, for the eastcoast domain, we analyzed two variable meshes with the same number of nodes; one using the $\lambda/\Delta x$ ratio and one based on the LTEA. Results show that the CM formulation is less sensitive to the meshing criteria, but that the LTEA reduces peak errors in the NCM formulation by two orders of magnitude (i.e., reduces it to the same as the CM formulation). Such a result is not surprising in that the LTEA method uses truncation error estimates from the velocity-based NCM equation.

4.4. Stability

Several numerical experiments were set up to examine the impact of the CM equation on stability, following the procedures discussed in Section 3.2. In all of the domains evaluated, results show no significant change in stability between the two algorithms, thus indicating that the CM equation does not influence stability.

4.5. Discussion

A broader look at the results of the previous sections suggests two trends. First, both the CM and NCM equations produce similar results in parts of the domain, e.g., in the deep water portion of the eastcoast domain, where the flow physics is nearly linear, neither the CM or NCM show large local mass balance errors (see Fig. 4a). But in regions of sharp bathymetric gradients, they differ significantly. In particular, note that the CM equation does not show the same local mass balance error spikes in these regions as does the NCM algorithm, as can been seen in Fig. 4a over the continental rise and Fig. 4b over the rise in bathymetry. It is precisely in these same regions where the non-linear advective terms are significant, so we will look for a correlation through simulation and analyses.

Second, the parallel behavior of the error in the local mass balance graph and the error in the local accuracy graph (cf. Figs. 4a and 5a) and the similar 3-peak pattern of the NCM results between Figs. 4b and 5b suggests that the two are related. In other words, can the finite volume method of computing mass balance serve as a surrogate variable for truncation error? This issue is also explored in this section.

To examine the behavior of the local truncation error for the advective terms further, we present the truncation error expressions for the advective terms in the NCM and CM equations below, as obtained from a Taylor Series expansion of the discrete equations. (The

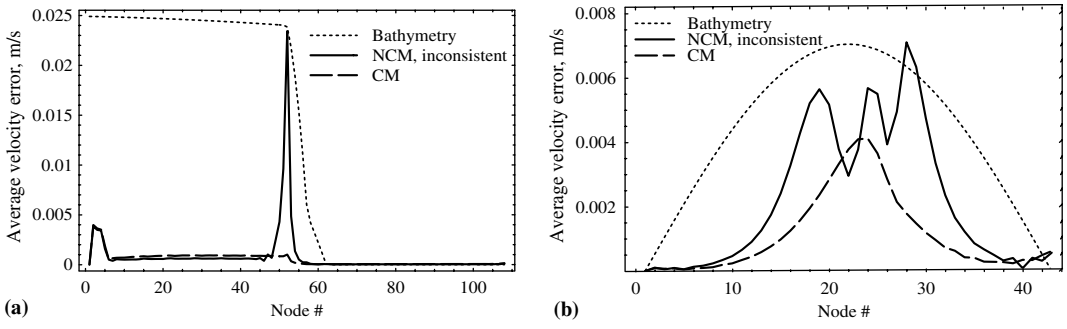

Fig. 5. Local spatial accuracy results (average velocity errors) for the (a) eastcoast and (b) sinusoidal domains. Legend is shown in the figure. Note that the bathymetry is not to scale. Nodal spacing is given in Table 1. Results utilized a variable nodal spacing with $\lambda/\Delta x = 300$.

full expansion is too lengthy to be repeated here, but the interested reader can find the results in Refs. [7,15].)

$$\mathrm{TE}_{\mathrm{NCM}}^{\mathrm{advective}} = \frac{1}{2}(\Delta x_{i+1} - \Delta x_i)\left[\left(\frac{\partial u_i}{\partial x}\right)^2 + \left(u_i \frac{\partial^2 u_i}{\partial x^2}\right)\right] - (\Delta x_i^2 - \Delta x_i \Delta x_{i+1} + \Delta x_{i+1}^2) \times \left[\frac{1}{2}\left(\frac{\partial u_i}{\partial x}\frac{\partial^2 u_i}{\partial x^2}\right) + \frac{1}{6}\left(u_i \frac{\partial^3 u_i}{\partial x^3}\right)\right] + \mathrm{H.O.T} \tag{10}$$

$$\mathrm{TE}_{\mathrm{CM}}^{\mathrm{advective}} = (\Delta x_{i+1} - \Delta x_i)\left[\left(\frac{\partial q_i}{\partial x}\frac{\partial u_i}{\partial x}\right) + \frac{1}{2}\left(u_i \frac{\partial^2 q_i}{\partial x^2} + q_i \frac{\partial^2 u_i}{\partial x^2}\right)\right] - \frac{1}{2}(\Delta x_i^2 - \Delta x_i \Delta x_{i+1} + \Delta x_{i+1}^2)\frac{\partial q_i}{\partial x}\frac{\partial^2 u_i}{\partial x^2} - \frac{1}{2}(\Delta x_i^2 - \Delta x_i \Delta x_{i+1} + \Delta x_{i+1}^2)\frac{\partial u_i}{\partial x}\frac{\partial^2 q_i}{\partial x^2} - \frac{1}{6}(\Delta x_i^2 - \Delta x_i \Delta x_{i+1} + \Delta x_{i+1}^2) u_i \frac{\partial^3 q_i}{\partial x^3} - \frac{1}{6}(\Delta x_i^2 - \Delta x_i \Delta x_{i+1} + \Delta x_{i+1}^2) q_i \frac{\partial^3 u_i}{\partial x^3} + \mathrm{H.O.T} \tag{11}$$

Note that the truncation error for each is formally first order accurate for unequal nodal spacing, but is second-order accurate for constant grid spacing, as would be expected for linear Galerkin finite elements. Because the flux varies more slowly than velocity in regions where the topography is changing rapidly, one would expect the magnitude of the derivatives of q, which appear in the CM truncation error expression, to be less than the corresponding derivatives of u, which appear in the NCM equation. To verify this, we carried out a scaling analysis of the leading error terms shown in Eqs. (10) and (11) using elevation and velocity values taken from eastcoast results over the continental rise (i.e., a region of high advection). After correcting for the differences in units between Eqs. (10) and (11) by dividing by the water column depth, we found that the truncation error for the CM advective terms is two orders of magnitude less than the corresponding terms for the NCM equation. In addition, if the scaling analysis is repeated for the deep water portion of the eastcoast domain, where the NCM and CM equations give similar results (i.e., a region of low advection, small flux and velocity gradients, and nearly linear physics), the two truncation error expressions scale to nearly identical values.

Physical arguments, simulations, and analysis thus lead us to believe that local truncation error is less for the CM equation than the NCM equation in regions of high advection. It then follows that the local mass balance error must also be less for the CM equation in these regions. To wit, in the limit as Δx and Δt tend toward zero, truncation error disappears and the discrete solution approaches the continuum solution (sans roundoff errors), so one would expect that local mass balance errors, as computed from direct integration of the continuum equations, would also tend toward zero. This is indeed the case. Increasing the resolution for simulation results shown in Fig. 4a and Fig. 5a decreases both the local spatial truncation error and the local mass balance error *at the same rate*.

If the advective terms do indeed dominate the error behavior (mass balance or spatial accuracy), one would expect less error if they were omitted from the equation (a quasi-linear simulation). The simulations used to produce Fig. 4a were re-run without these advective terms; the results show that the peak local mass balance errors are 40% less than those shown in Fig. 4a. In addition, if one removes the remaining non-linear terms from the equations and runs a full linear simulation, the local mass balance errors diminish only slightly from simulations with just the advective terms excluded, thus suggesting that the advective terms are the primary contributor to errors in these regions.

All of this leads us to conclude that the choice of dependent variable (flux vs. velocity) *and* the form of the advective terms (conservative vs. non-conservative) in the discrete equations are the primary causes for the difference in behavior between the NCM and CM simulations, with the CM equation offering increased accuracy in areas with high advective gradients. Furthermore, local mass balance error, when measured by direct integration of the continuity equation, parallels local truncation error and can thus be used as a surrogate variable for local truncation error. As such, among other applications, it can be used to identify regions where mesh refinement is necessary. Such a conclusion is also consistent with earlier studies [14]. It remains to be demonstrated in this paper that these 1D observations carry over to 2D simulations.

5. Two-dimensional numerical experiments

5.1. Domains evaluated

In 2D, we examined the behavior of the two formulations of the momentum equation on the quarter annular harbor (denoted "quarter annular"), a fictional grid that has a well-documented analytical solution, and several application domains—Bight of Abaco (denoted "Bahamas"), Western North Atlantic (denoted "WNAT"), Gulf of Mexico, and Persian Gulf.

The quarter annular grid is shown in Fig. 6. Boundaries are marked in the figure, with either ocean or land indicated. The boundary condition for the open ocean boundary is the M_2 tidal constituent with a 1-m amplitude, while the land boundaries are no flow. For the experiments herein, we utilized a 10×10 resolution (radial divisions $\times$ θ divisions), which gives a $\lambda/\Delta x$ of 26, an

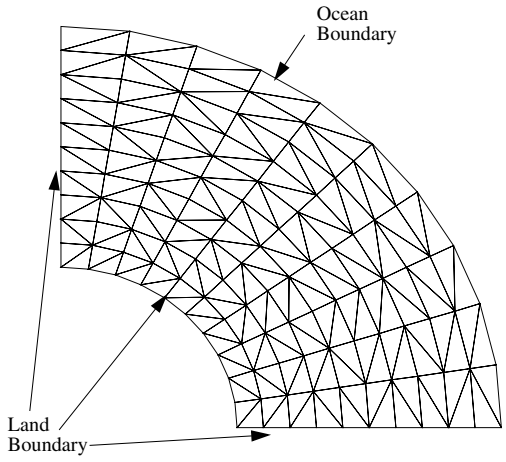

Fig. 6. Quarter annular harbor domain (10 × 10 resolution).

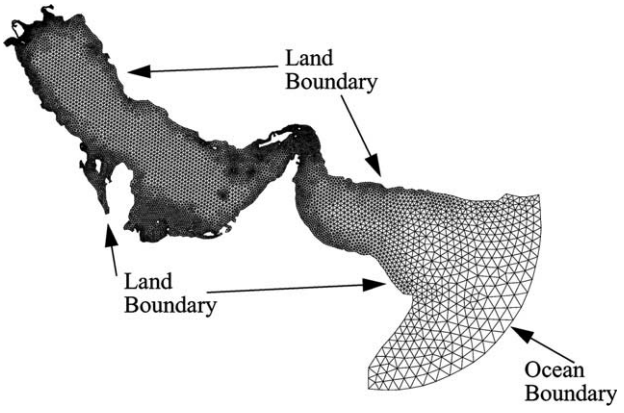

Fig. 7. Persian Gulf domain.

accepted value in practice [17]. Bathymetry varies from a minimum of 3 m to a maximum of 19 m with the inner radius at a distance of 60,690 m and the outer radius at a distance of 152,400 m.

Fig. 7 shows the Persian Gulf domain, while the three other application domains (WNAT, Gulf of Mexico and Bahamas) are shown in Fig. 8. Boundary conditions are indicated in the figures. Table 2 contains information regarding parameters, boundary and grid data for each of the application domains (i.e., number of nodes, range of nodal spacing, etc.). In all of the domains, the land boundaries are treated as no flow and the ocean boundaries utilize the tidal constituents presented in Table 2.

5.2. Mass conservation

5.2.1. Global mass conservation

We analyzed the impact of the CM equation on global mass balance errors utilizing the procedures presented in Section 3.1. Results are shown in Fig. 9, which shows the average error over time for both formulations of the momentum equation. (Recall that throughout this 2D section, the NCM advective terms are consistent with the GWC equation.) The CM results show slight to moderate decreases in the global mass conservation errors in four of the domains. In two domains, the WNAT and the Gulf of Mexico (LTEA resolution), we observe that the NCM equation produces slightly better or similar results to the CM equation. In the WNAT domain, the similar error behavior is due to the fact that the majority of the domain is in deeper water where the non-linear terms do not play a significant role; these 2D WNAT results parallel the 1D results for the eastcoast slice (cf. Fig. 3) with the consistent treatment of the advective terms.

Regarding the Gulf of Mexico results, we note that the LTEA method provides extra resolution on the shelf break [8,9]. This extra shelf resolution decreases the global mass error in the NCM equation results. On the other hand, the CM equation results are only slightly less than the $\lambda/\Delta x$ resolution (Fig. 9, Gulf of Mexico open bars), which indicates that the CM equation is less sensitive to the method of node placement on the shelf. Such behavior is consistent with the 1D experiments and consistent with the fact that the LTEA uses the velocity-based NCM truncation errors to determine node placement.

5.2.2. Local mass conservation

Next we analyzed the impact of the CM equation on local mass conservation utilizing the procedures presented in Section 3.1. Results are presented as contour plots in Fig. 10 with the *difference* in the mass balance errors shown on the log scale. In Fig. 10, we include the bathymetric contours to indicate where the steep bathymetry gradients occur. Results indicate that the CM equation reduces the local mass balance errors over a significant portion of the domain, with the largest gains occurring in the shelf and shelf break regions. (Observe the relative amount of blue in the graphs.) This is most evident in Fig. 10c (WNAT), where we see decreases in local mass balance errors (indicated by the blue area in the graph) with the CM equation along the continental shelf and shelf break region in the Gulf of Mexico and along the eastern seaboard of the United States. In the WNAT and Gulf of Mexico (LTEA resolution) domains, we find that the differences in local mass balance errors between the two formulations indicate NCM local mass balance errors are less along the ocean boundaries; land boundaries near the ocean boundary also have high local mass balance errors that decrease as one moves away from the ocean boundary. These results parallel the 1D observations.

We analyzed the influence of the meshing criteria on local mass balance errors in the Gulf of Mexico by using the LTEA method to provide extra shelf resolution. (Re-

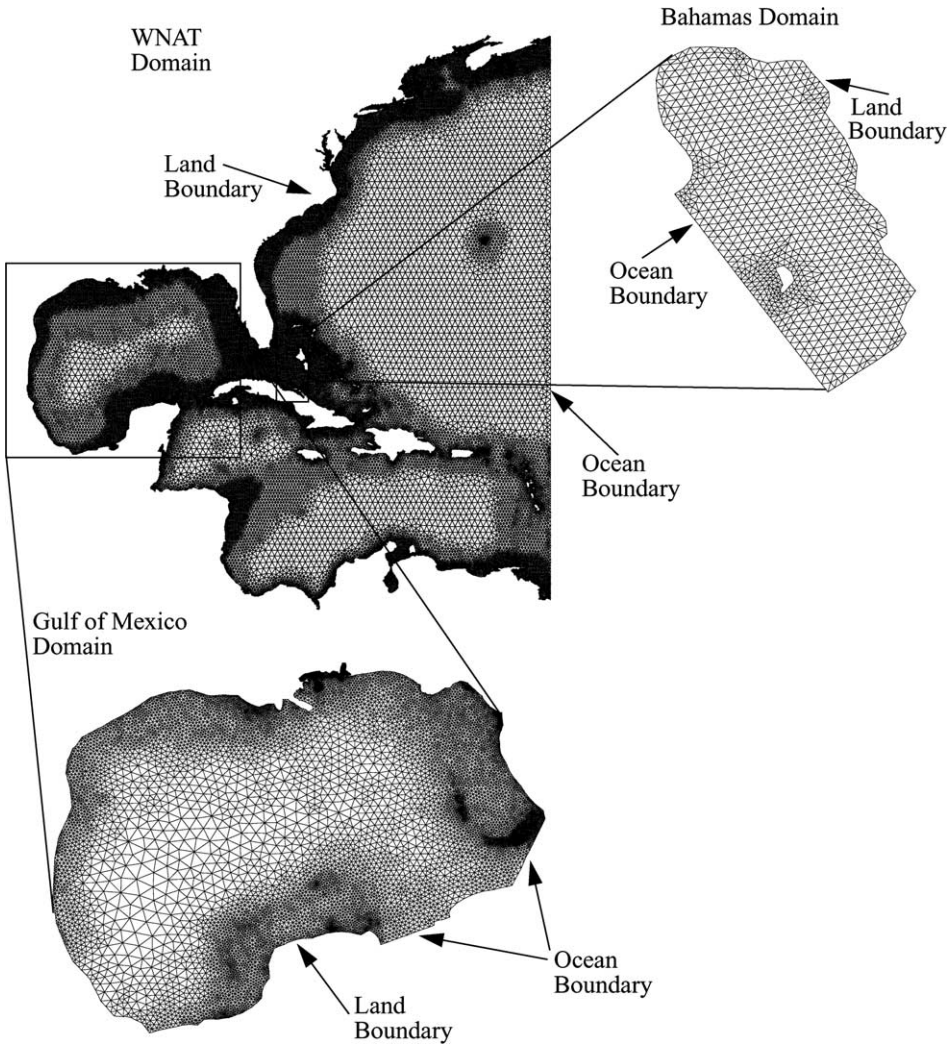

Fig. 8. WNAT domain with the Gulf of Mexico and Bahamas domains zoomed in.

Table 2
Application domain information

	Bahamas	Gulf of Mexico		WNAT	Persian Gulf
Meshing criteria	$\lambda/\Delta x$	$\lambda/\Delta x$	LTEA	$\lambda/\Delta x$	$\lambda/\Delta x$
# nodes	926	11,701	11,934	32,947	8550
# elements	1696	21,970	22,870	61,705	15,724
Min. Bathymetry (m)	1.0	1.0	0.7	3.0	1.0
Max. Bathymetry (m)	≈9.0	≈3600.0	≈3600.0	≈6000.0	≈3700.0
Range of nodal spacing (km)	0.8–2.8	1–140	1–72	8–32	1–40
G value (s^{-1})	0.009	0.009	0.009	0.005	0.01
M_2 amplitude (m)	0.395	0.07–0.173	0.07–0.173	0.0652–0.5580	0.496–0.6517
O_1 amplitude (m)	0.075	NA	NA	NA	0.185–0.194
K_1 amplitude (m)	0.095	NA	NA	NA	0.35–0.37
S_2 amplitude (m)	0.06	NA	NA	NA	0.193–0.256
N_2 amplitude (m)	0.10	NA	NA	NA	0.115–0.149
Q_1 amplitude (m)	NA	NA	NA	NA	0.0036–0.0037
P_1 amplitude (m)	NA	NA	NA	NA	0.113–0.118
K_2 amplitude (m)	NA	NA	NA	NA	0.0042–0.0058

call from Table 2 that the total number of nodes is approximately the same.) As can be seen in Fig. 10a and 10b, the CM equation produces less error than the NCM equation, regardless of meshing technique. This is notable because the LTEA method is designed to reduce truncation errors for velocity-based solutions.

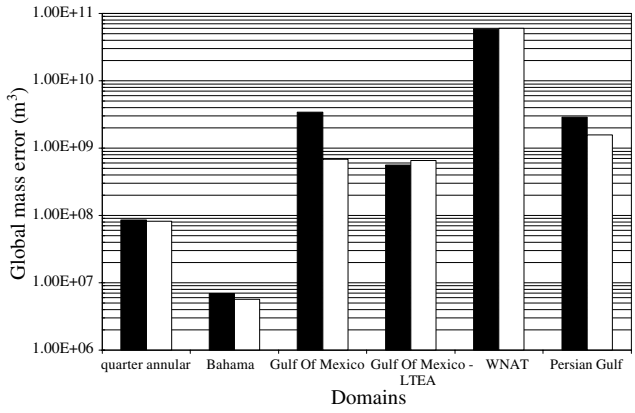

Fig. 9. Global mass conservation results for the domains analyzed. Plot of the average global mass errors for both forms of the momentum equation (open bars—conservative momentum, filled bars—non-conservative momentum).

5.3. Spatial accuracy

Results from the 1D spatial accuracy experiments indicate that the CM equation does not impact the global spatial accuracy significantly; therefore, we only analyze local spatial accuracy for the 2D domains.

We evaluated the effect of the CM equation on local spatial accuracy using CAFE curves [16]. Only the fictitious quarter annular domain was studied because the bathymetry is known from an analytical equation at all spatial locations. (For real domains, bathymetry is known only at discrete points from field measurements. To interpolate between these as the grid is refined introduces additional noise besides truncation errors into the measured response, so that spatial resolution studies are inconclusive). Procedures followed in this section are presented in Section 3.3.3. To obtain the "true solution", we refined the quarter annular domain until the convergence criteria was met, which resulted in a resolution of 200×200. Note that CM vs. NCM solutions are nearly indistinguishable at this fine resolution ($\lambda/\Delta x$ ratio over 500).

Tables 3 and 4 present a snapshot of the error levels obtained from the CAFE analysis for the quarter annular domain comparing coarse and fine ("true") resolutions. Spatial resolution is indicated in the tables. The values in bold type highlight which form of the

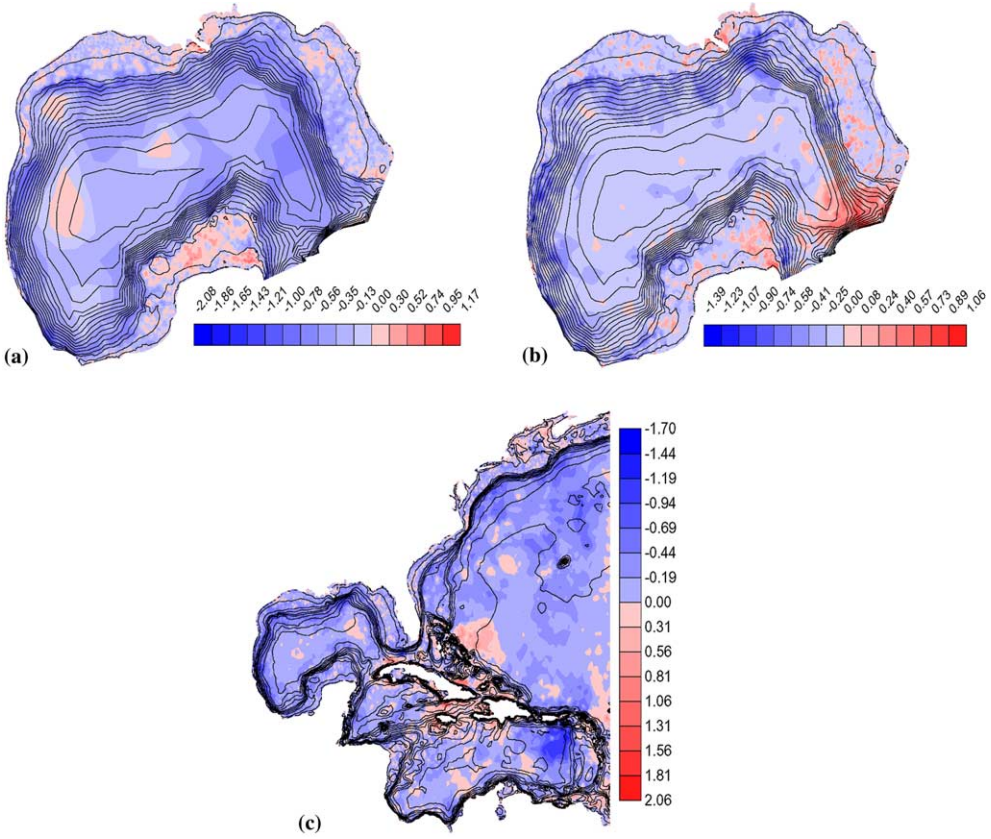

Fig. 10. Local mass conservation results for the Gulf of Mexico and WNAT domains: (a) GOM—$\lambda/\Delta x$, (b) GOM—LTEA and (c) WNAT—$\lambda/\Delta x$. Red coloring indicates where the NCM equation results are better while the blue coloring indicates where the CM equation results are better. The legend shows the difference between the CM and NCM results on a log scale.

Table 3
Elevation error measures

	Quarter annular	
	NCM	CM
Resolution comparison	10×10 vs. 200×200	10×10 vs. 200×200
Elevation amplitude (absolute)		
% Exceeding −0.0015 m (−0.005 ft)	8.4	**1.2**
% Exceeding 0.0015 m (0.005 ft)	1.3	**0.56**
% Exceeding ±0.0015 m (±0.005 ft)	9.7	**1.8**
Elevation amplitude (relative)		
% Exceeding −0.5%	0.12	**<0.001**
% Exceeding 0.5%	0.51	**0.051**
% Exceeding ±0.5%	0.63	**0.051**
Elevation phase difference		
% Exceeding −0.2°	14	**0.0083**
% Exceeding 0.2°	2.6	**2.5**
% Exceeding ±0.2°	17	**2.5**

Table 4
Velocity error measures

	Quarter annular	
	NCM	CM
Resolution	10×10 vs. 200×200	10×10 vs. 200×200
Major semi-axis (absolute)		
% Exceeding −0.015 m s^{-1} (−0.05 ft s^{-1})	**0.66**	1.0
% Exceeding 0.015 m s^{-1} (0.05 ft s^{-1})	**0.0062**	0.054
% Exceeding ±0.015 m s^{-1} (±0.05 ft s^{-1})	**0.67**	1.1
Major semi-axis (relative)		
% Exceeding −1%	**75**	78
% Exceeding 1%	19	**15**
% Exceeding ±1%	94	**93**
Major semi-axis phase difference		
% Exceeding −10°	**0.086**	0.092
% Exceeding 10°	0.14	**0.13**
% Exceeding ±10°	0.23	**0.22**
Eccentricity		
% Exceeding −0.1	0.29	**0.23**
% Exceeding 0.1	**0.040**	0.19
% Exceeding ±0.1	**0.33**	0.42
Major semi-axis direction		
% Exceeding −5°	**1.3**	1.4
% Exceeding 5°	0.23	**0.19**
% Exceeding ±5°	**1.5**	1.6

momentum equation provides the least error. This data, combined with an analysis of the full CAFE plots (not shown), reveals that the CM equation significantly improves the elevation response over the entire domain. For four of the five velocity components, the CM and NCM algorithms have very similar errors, while for one velocity component (major semi-axis, absolute), NCM is better over much of the domain. Altogether, the CM algorithm shows improved local spatial accuracy.

5.4. Stability

Lastly, we analyzed the impact of the CM equation on stability using the procedures presented in Section 3.2. Results for all of the domains show no impact on stability due to the CM equation. In fact, we found that the two momentum equations produced a nearly identical maximum allowable time step. Therefore, the CM equation does not influence stability, a result that is similar to the 1D findings.

6. Conclusions

Herein, we analyzed the impact of using the flux-based, conservative form of the momentum equation instead of the velocity-based, non-conservative form to compute the depth-averaged velocities in 1D and 2D GWC-based shallow water models. Our hypothesis in this study was that the use of the conservative momentum equation would improve both global and local mass conservation, eliminate the need to reformulate the advective terms between the GWC and NCM equations, and lessen the need for extensive refinement in areas with steep bathymetry gradients. Through a set of extensive numerical experiments, supported with truncation error analysis, we show that the use of the conservative momentum equation does improve global mass conservation in most simulations, and it greatly improves local mass conservation in regions of steep topography for all of the domains, as measured in the finite volume sense. Paralleling the local mass balance results, local spatial accuracy also improves. The analysis in Section 4.5 demonstrates that both the choice of dependent variable and the form of the advective terms in the discrete equations causes a difference in behavior between the NCM and CM simulations, with the CM equation offering increased accuracy in areas of high advective gradients. Also, local mass balance error, when measured by direct integration of the primitive continuity equation, parallels local truncation error and can thus be used as a surrogate variable for local truncation error. As such, among other applications, it can be used to identify regions where mesh refinement is necessary. Furthermore, the use of the conservative form of the momentum equation eliminates the need for reformulating the advective terms between the governing equations. However, results are inconclusive regarding the third hypothesis, that is, for some simulations the LTEA mesh does not impact the CM results, while in others the LTEA mesh reduces both NCM and CM local mass balance errors.

In the end, the significant decrease in local mass balance error and corresponding increase in local spatial accuracy for the CM formulation, with no loss of global spatial accuracy and stability, provides sufficient

evidence for its use in GWC-based, finite element shallow water models.

Acknowledgments

Financial support for this research was provided in part by the National Science Foundation under contract ACI-9623592, the United States Department of Education GAANN Fellowship, and the Department of Defense under contract ONR N00014-02-1-0651. Any opinions, findings and conclusions or recommendations expressed in this material are those of the authors and do not necessarily reflect those of the funding agencies. We thank the anonymous reviewers for their constructive comments.

References

[1] Aldama AA, Aguilar A, Kolar RL, Westerink JJ. A mass conservation analysis of the GWCE formulation. In: Bentley LR, et al., editors. Computational methods in water resources XIII. Computational methods, surface water systems and hydrology, vol. 2. Rotterdam/Brookfield: A.A. Balkema; 2000. p. 907–12.

[2] Berger RC, Howington M. Discrete fluxes and mass balance in finite elements. J Hyd Res 2002;128(1):87–92.

[3] Blain CA, Westerink JJ, Luettich RA. Grid convergence studies for the prediction of hurricane storm surge. Int J Numer Methods Fluids 1998;26:369–401.

[4] Dawson C, Proft J. Discontinuous and coupled continuous/discontinuous Galerkin methods for shallow water equations. Comput Methods Appl Mech Eng 2002;191:4721–46.

[5] Dawson C, Proft J. Coupled discontinuous and continuous Galerkin finite element methods for the shallow water equations. Comput Methods Appl Mech Eng 2004;193:289–318.

[6] Dresback KM, Kolar RL, Dietrich JC. A 2D implicit time-marching algorithm for shallow water models based on the generalized wave continuity equation. Int J Numer Methods Fluids 2004;45:253–74.

[7] Dresback KM, Kolar RL. Truncation error analysis of ADCIRC. EM/GIS Technical Report #04-02, 2004. Available from: http://www.coe.ou.edu/emgis/kolar/pages/reports.html.

[8] Hagen SC, Westerink JJ, Kolar RL. One-dimensional finite element grids based on a localized truncation error analysis. Int J Numer Methods Fluids 2000;32:241–61.

[9] Hagen SC, Westerink JJ, Kolar RL. Two-dimensional, unstructured mesh generation for tidal models. Int J Numer Methods Fluids 2001;35:669–86.

[10] Hughes TJR, Engel G, Mazzei L, Larson MG. The continuous Galerkin method is locally conservative. J Comput Phys 2000;163(2):467–88.

[11] Kinnmark IPE. The shallow water wave equations: formulations, analysis and application. Lecture notes in engineering, vol. 15. Berlin: Springer-Verlag; 1986.

[12] Kolar RL, Gray WG, Westerink JJ. An analysis of the mass conserving properties of the generalized wave continuity equation. In: Russel TF, et al., editors. Computational methods in water resources IX. Mathematical modeling in water resources, vol. 2. Southampton/London: Computational Mechanics/Elsevier; 1992. p. 537–44.

[13] Kolar RL, Gray WG, Westerink JJ. Boundary conditions in shallow water models—an alternative implementation for finite element codes. Int J Numer Methods Fluids 1996;22(7):603–18.

[14] Kolar RL, Westerink JJ, Cantekin ME, Blain CA. Aspects of nonlinear simulations using shallow-water models based on the wave continuity equation. Comp Fluids 1994;23:523–8.

[15] Kolar RL, Westerink JJ, Hagen SC. Truncation error analysis of shallow water models based on the generalized wave continuity equation. In: Aldama AA, et al., editors. Computational methods in water resources IX. Mathematical modeling in water resources, vol. 2. Southampton/London: Computational Mechanics/Elsevier; 1996. p. 215–22.

[16] Luettich RA, Westerink JJ. Continental shelf scale convergence studies with a tidal model. In: Lynch DR, Davies AM, editors. Quantitative skill assessment for coastal ocean models, vol. 47. Washington, DC: American Geophysical Union; 1995. p. 349–71.

[17] Luettich RA, Westerink JJ, Scheffner NW. ADCIRC: an Advanced Three-Dimensional Circulation Model for Shelves, Coasts and Estuaries; Report 1: Theory and Methodology of ADCIRC-2DDI and ADCIRC-3DL, Technical Report DRP-92-6, Department of the Army, USACE, 1992.

[18] Lynch DR, Gray WG. A wave equation model for finite element tidal computations. Comp Fluids 1979;7(3):207–28.

[19] Lynch DR, Holboke MJ. Normal flow boundary conditions in 3D circulation models. Int J Numer Methods Fluids 1997;25(10):1185–205.

[20] Walters RA, Carey GF. Numerical noise in ocean and estuarine models. Adv Water Resour 1984;7:15–20.